

# SmartMeterFM: Unifying Smart Meter Data Generative Tasks Using Flow Matching Models

Nan Lin, *Graduate Student Member, IEEE*, Yanbo Wang *Graduate Student Member, IEEE*,  
 Jacco Heres, Peter Palensky, *Senior Member, IEEE*, Pedro P. Vergara, *Senior Member, IEEE*

**Abstract**—Smart meter data is the foundation for planning and operating the distribution network. Unfortunately, such data are not always available due to privacy regulations. Meanwhile, the collected data may be corrupted due to sensor or transmission failure, or it may not have sufficient resolution for downstream tasks. A wide range of generative tasks is formulated to address these issues, including synthetic data generation, missing data imputation, and super-resolution. Despite the success of machine learning models on these tasks, dedicated models need to be designed and trained for each task, leading to redundancy and inefficiency. In this paper, by recognizing the powerful modeling capability of flow matching models, we propose a new approach to unify diverse smart meter data generative tasks with a single model trained for conditional generation. The proposed flow matching models are trained to generate challenging, high-dimensional time series data, specifically monthly smart meter data at a 15 min resolution. By viewing different generative tasks as distinct forms of partial data observations and injecting them into the generation process, we unify tasks such as imputation and super-resolution with a single model, eliminating the need for re-training. The data generated by our model not only are consistent with the given observations but also remain realistic, showing better performance against interpolation and other machine learning based baselines dedicated to the tasks.

## I. INTRODUCTION

Ensuring the safe and reliable operation of the electrical grid critically depends on accurate and timely monitoring of system states. Smart meters and other sensing devices provide valuable data that enable grid operators to assess asset conditions [1], detect contingencies [2], and support advanced control strategies [3]. In practice, however, data availability remains a major challenge. Many assets are only partially monitored due to limited smart meter deployment and privacy restrictions. The privacy and commercial sensitivity of smart meter data also prevent distribution system operators (DSOs) from sharing data [4]. Furthermore, the available data are often incomplete, noisy, or insufficiently granular. For instance, missing values arise from sensor or communication failures, while limited deployments lead to partial observability. Additionally, many applications require measurements at

Nan Lin is funded by NWO Align4Energy Project NWA.1389.20.251.

Nan Lin, Peter Palensky, and Pedro P. Vergara are with the Intelligent Electrical Power Grids Group, Delft University of Technology, 2628 CD Delft, The Netherlands; Yanbo Wang is with the Signal Processing Systems Group, Delft University of Technology; Jacco Heres is with Alliander N.V., 6812 AH Arnhem, The Netherlands (e-mail: N.Lin@tudelft.nl, P.Palensky@tudelft.nl, P.P.VergaraBarrios@tudelft.nl, Y.Wang-27@tudelft.nl, jacco.heres@alliander.com).

The code for models and experiments used in this paper can be found in Github Repositories: <https://github.com/sentient-codebot/SmartMeterFM> and <https://github.com/distributionnetworksTUDelft/SmartMeterFM>

a finer temporal resolution than those provided by sensors. Addressing these challenges typically involves tasks such as imputing missing values, enhancing measurement resolution, or generating realistic and plausible operation scenarios conditioned on categorical or continuous variables.

Conditional data generation plays a central role in smart grid applications, enabling operators to simulate realistic operating scenarios for planning and risk assessment [5]. A variety of models have been proposed for this purpose, including statistical approaches such as t-Copula [6], deep generative models such as variational autoencoder [7], adversarial frameworks such as generative adversarial networks (GANs), particularly the Wasserstein GAN with gradient penalty (WGAN-GP) [8], diffusion-based models [9], [10]. Despite their successes, these approaches face significant challenges. Statistical models such as the t-Copula scale poorly to high-dimensional time series data, such as monthly 15 min load profiles with up to 2976 time steps. VAEs often suffer from distribution shift and posterior collapse, leading to degraded sample quality [11]. GAN-based methods, while powerful, are notoriously difficult to train and vulnerable to mode collapse, resulting in limited diversity. Diffusion-based models, such as Physics-Informed Diffusion Models [10] and EnergyDiff [9], are easy to train and can generate high-quality data. However, neither of the previous deep generative models can adapt to new conditions without re-training.

Furthermore, recent comparative studies [12] highlight that most existing approaches struggle with complex conditioning, particularly involving mixed categorical and continuous inputs. These limitations indicate that current conditional generation techniques are insufficient for the diverse and high-dimensional data challenges encountered in grid operation and planning.

Besides data generation, data imputation is also crucial in distribution network planning and operation, where missing values often result from meter malfunctions or communication failures. Traditional methods, such as linear or spline interpolation, can provide quick fixes but typically fail to recover the dynamics and extreme values, which are essential for accurate load monitoring [13], [14] and anomaly detection [15]. To address these shortcomings, supervised machine learning approaches have been introduced. For example, the GAN-based model proposed in [16] trains predictive models to infer missing values from observed data and incorporates specialized loss functions to recover the peak values. Nevertheless, such models remain limited in practice. They generate overly smooth reconstructions that underestimate the peak values, and their task-specific training makes it difficult to adapt to

different patterns of missing data.

Super-resolution is another critical task in grid data analytics, aiming to recover high-frequency profiles from coarse-resolution measurements. Accurate up-sampling is valuable for applications such as demand response and load aggregation, where fine-grained temporal information is required but often unavailable due to limited metering infrastructure [17]. Traditional interpolation techniques can produce smoothed signals but generally fail to capture realistic high-frequency variations [18]. Recently, deep generative models have been explored for this task. For example, the model in [19] employs a GAN to generate realistic high-resolution load profiles and has demonstrated promising performance. However, in practice, GAN-based models are difficult to train due to instability and potential mode collapse, and once trained, they are tied to a fixed scale factor. For instance, a model trained to up-sample 30 min data into 15 min resolution cannot be applied to convert 1 h profiles. This highlights a broader issue: existing imputation and super-resolution methods remain specialized solutions that lack versatility and adaptability across different missing patterns and scales.

The above-discussed tasks can be collectively viewed as *generative data tasks*, since they all aim to synthesize realistic smart meter data that respects the intrinsic patterns of consumption and generation while satisfying conditions (e.g., customer category) or constraints (e.g., peak demand equal to a measured value). Despite this shared essence, existing methods are typically designed for a single task, limiting their versatility and scalability. To overcome this fragmentation, we introduce *SmartMeterFM*, a unified flow matching model for smart meter data generative tasks. Flow matching (FM), originally developed for image generation [20], is a powerful class of generative models that learns a probability flow ordinary differential equation to approximate a complex data distribution. Compared to diffusion models, which have also shown promise for smart meter data generative tasks [9], FM models offer a simpler mathematical formulation, faster sampling, and comparable generation quality [21]. *SmartMeterFM* adapts FM to the time series domain, where it is trained once on conditional generation and, through inference-time guidance, seamlessly adapts to imputation and super-resolution tasks without re-training.

The main contributions of this paper are as follows:

- We propose *SmartMeterFM*, a novel flow matching model for conditional generation of smart meter data, capable of generating high-dimensional monthly 15 min resolution profiles with high fidelity. A tailored Transformer-based architecture enables the model to handle variable-length sequences, allowing different months to be modeled by a single framework.
- We demonstrate that *SmartMeterFM* can also unify multiple generative tasks, namely generation conditioning on categorical variables, generation conditioning on peak and total consumption, imputation, and super-resolution, by training solely on conditional generation and applying task-specific inference-time guidance. Without additional re-training, *SmartMeterFM* outperforms specialized su-

pervised learning baselines, achieving superior quantitative accuracy while preserving the fidelity of the data.

## II. FLOW MATCHING WITH INFERENCE TIME GUIDANCE

Flow Matching (FM) is a generative modeling framework that trains Continuous Normalizing Flows (CNF) to synthesize complex data distributions [20]. Compared to diffusion models, FM offers a simpler mathematical formulation and faster sampling while maintaining high generation quality [21]. In this section, we outline the FM formulation and propose an inference-time guidance mechanism that enables a single trained model to adapt to various generative tasks, such as imputation and super-resolution, without re-training.

### A. Problem Formulation

Consider a dataset of smart meter measurements  $\{x^{(i)}\}_{i=1}^N$ , where each  $x^{(i)} \in \mathbb{R}^T$  represents a time-series profile sampled from an unknown distribution  $q(x)$ . The dimension  $T$  is determined by the resolution and duration; for example, a monthly profile at 15 min resolution implies  $T \approx 3000$ . Modeling the high-dimensional distribution  $q(x)$  directly is computationally challenging.

To address this, we seek a time-dependent mapping that transforms a simple prior distribution  $p(x) = \mathcal{N}(0, I)$  into the complex data distribution  $q(x)$ . We model this transformation using an Ordinary Differential Equation (ODE) over an auxiliary time variable  $t \in [0, 1]$ :

$$\frac{dx_t}{dt} = u_t(x_t), \quad x_0 \sim p(x), \quad (1)$$

where  $x_t$  is the state at time  $t$ , and  $u_t(\cdot)$  is a velocity field. Integrating this ODE from  $t = 0$  (noise) to  $t = 1$  (data) generates a sample:

$$x_1 = x_0 + \int_0^1 u_t(x_t) dt. \quad (2)$$

If the velocity field  $u_t$  is properly defined, the terminal state  $x_1$  follows the target distribution  $q(x)$ . The goal of Flow Matching is to learn a neural network  $u_\theta(x, t)$  that approximates this optimal velocity field.

### B. Training via Conditional Flow Matching

Training a CNF by directly maximizing log-likelihood is unstable and computationally expensive due to the need for Jacobian trace estimations [22]. FM overcomes this by defining a specific, tractable target probability path.

We construct a path that transforms noise  $x_0$  to data  $x_1$  via linear interpolation:

$$x_t = tx_1 + (1 - t)x_0. \quad (3)$$

Differentiating (3) with respect to time yields the target velocity for a specific data-noise pair:

$$\dot{x}_t = x_1 - x_0. \quad (4)$$

Intuitively, this target velocity pulls the sample along a straight line from the noise distribution to the data distribution. To train the model, we regress the neural network  $u_\theta(x, t)$  to match

**Algorithm 1** Training CNF with Flow Matching

---

**Require:** Dataset  $\mathcal{D} = \{(x_1^{(i)}, y^{(i)})\}_{i=1}^N$ , velocity network  $u_\theta$

- 1: **while** not converged **do**
- 2:   Sample mini-batch  $\mathcal{B} \subset \mathcal{D}$
- 3:   **for**  $(x_1, y) \in \mathcal{B}$  **do**
- 4:     Sample  $t \sim \mathcal{U}(0, 1)$ ,  $x_0 \sim \mathcal{N}(0, I)$
- 5:     Set  $x_t \leftarrow tx_1 + (1-t)x_0$
- 6:   **end for**
- 7:   Update  $\theta$  by gradient descent on  $\frac{1}{|\mathcal{B}|} \sum \|u_\theta(x_t, t, y) - (x_1 - x_0)\|_2^2$
- 8: **end while**

---

this target direction. The loss function is the expectation of the mean squared error over all data points  $x_1 \sim q(x)$ , noise samples  $x_0 \sim p(x)$ , and time steps  $t \sim \mathcal{U}(0, 1)$ :

$$\mathcal{L}(\theta) = \mathbb{E}_{t, x_0, x_1} \left[ \|u_\theta(x_t, t) - (x_1 - x_0)\|_2^2 \right]. \quad (5)$$

This objective is convex with respect to  $u_\theta(x_t, t)$  and numerically stable. By minimizing (5) using stochastic gradient descent, the network  $u_\theta$  learns the average velocity field required to transport the Gaussian prior to the smart meter data distribution. Once trained, new samples are generated by drawing  $x_0 \sim \mathcal{N}(0, I)$  and numerically integrating (1) using an ODE solver.

### C. Conditional Flow Matching

Conditional generation means sampling from the posterior distribution  $q(x|y)$ , where  $y$  is a condition. Let  $p_t(x_t)$  denote the distribution of state  $x_t$  at time  $t$  induced by the ODE, with  $x_0 \sim p(x_0)$  and  $x_1 \sim q(x_1)$ . The continuity equation [23], [20] yields<sup>1</sup>

$$u_t(x_t) = a_t x_t + b_t \nabla_{x_t} \log p_t(x_t), \quad (6)$$

where  $a_t = \frac{1}{t}$  and  $b_t = \frac{1-t}{t}$ . Replacing  $\nabla_{x_t} \log p_t(x_t)$  with  $\nabla_{x_t} \log p_{t|y}(x_t|y)$  yields the conditional velocity

$$u_t(x_t|y) = a_t x_t + b_t \nabla_{x_t} \log p_{t|y}(x_t|y) \quad (7)$$

$$= a_t x_t + b_t (\nabla_{x_t} \log p_t(x_t) + \nabla_{x_t} \log p_{y|t}(y|x_t)) \quad (8)$$

$$= u_t(x_t) + b_t \nabla_{x_t} \log p_{y|t}(y|x_t). \quad (9)$$

The conditional velocity thus comprises two components: the unconditional velocity and a guidance term  $b_t \nabla_{x_t} \log p_{y|t}(y|x_t)$ . Following this gradient steers  $x_t$  toward satisfying the condition  $y$ .

This formulation suggests two approaches for incorporating conditions:

- 1) **Direct parameterization:** Model the conditional velocity  $u_t(x_t|y) \approx u_\theta(x_t, t, y)$  directly. This approach supports arbitrary conditions  $y$  without requiring prior knowledge of how  $y$  relates to  $x$ , but the dependence on  $y$  must be learned through training. The condition  $y$  becomes a mandatory input to the model.

<sup>1</sup>At  $t = 0$ , singularities arise and require special treatment [20]. In practice, we approximate  $t = 0$  with  $t = 10^{-3}$ .

- 2) **Guidance parameterization:** Model only the unconditional velocity  $u_\theta(x_t, t)$  and derive the guidance term analytically. This requires knowing the functional relationship between  $x$  and  $y$ , but allows conditions to be added dynamically at inference time without re-training. We refer to this as *inference time guidance*.

These two methods can be combined when complex conditions arise. Let  $y = [y_1, y_2]$ , where  $y_1$  is handled through direct parameterization and  $y_2$  through inference time guidance. The velocity becomes

$$u_t(x_t|y_1, y_2) = a_t x_t + b_t \nabla_{x_t} \log p_{t|y_1, y_2}(x_t|y_1, y_2) \quad (10)$$

$$= a_t x_t + b_t [\nabla_{x_t} \log p_{t|y_1}(x_t|y_1) + \nabla_{x_t} \log p_{y_2|t, y_1}(y_2|x_t, y_1)] \quad (11)$$

$$= u_t(x_t|y_1) + b_t \nabla_{x_t} \log p_{y_2|t, y_1}(y_2|x_t, y_1) \quad (12)$$

$$= u_t(x_t|y_1) + b_t \nabla_{x_t} \log p_{y_2|t}(y_2|x_t) \quad (13)$$

$$\approx u_\theta(x_t, t, y_1) + b_t \nabla_{x_t} \log p_{y_2|t}(y_2|x_t). \quad (14)$$

Equation (13) holds when  $y_1$  and  $y_2$  are conditionally independent given  $x_t$ , which is true at  $t = 1$  for any quantity deterministically related to the data. For instance, once the smart meter data  $x$  is known, total consumption ( $y_2$ ) is fully determined and thus independent of other conditions. Near  $t = 0$ , slight correlations may exist but are negligible in practice.

For direct parameterization, we feed  $y_1$  to  $u_\theta(x_t, t, y_1)$  during training. The loss function becomes

$$\tilde{\mathcal{L}}(\theta) = \mathbb{E}_{x_0, (x_1, y_1)} \left[ \|u_\theta(x_t, t, y_1) - (x_1 - x_0)\|_2^2 \right], \quad (15)$$

where  $x_0 \sim p(x_0)$  is independent of  $(x_1, y_1)$ , which are sampled jointly from real data. The training procedure is summarized in Algorithm 1.

### D. Inference Time Guidance

Inference time guidance enables training *one* model and adapting it to many tasks without re-training. We now derive this guidance term.

Denote the guidance term from (9) as

$$g_t := b_t \nabla_{x_t} \log p_{y|t}(y|x_t). \quad (16)$$

We consider conditions with a deterministic functional relationship  $y = f(x_1)$ . Conditioning on  $y$  restricts sampling to the preimage  $\Omega(y) = f^{-1}(y) = \{x \in \mathbb{R}^d | f(x) = y\}$ .

Since  $p_{y|1}(y|x_1) = \delta(y - f(x_1))$  has undefined gradient, we introduce small Gaussian noise:

$$y = f(x_1) + n, \quad n \sim \mathcal{N}(0, \epsilon^2 I), \quad (17)$$

where  $\epsilon$  is a small positive number. Let  $\psi_{1|t}(x_t)$  denote the mapping from  $x_t$  to  $x_1$  via the ODE. With  $x_1 = \psi_{1|t}(x_t)$ , the guidance becomes

$$g_t = \frac{b_t}{\epsilon^2} J_f^T(x_t) J_f^T(x_1)(y - f(x_1)). \quad (18)$$

The term  $\frac{1}{\epsilon^2} J_f^T(x_1)(y - f(x_1))$  is the Gauss-Newton direction for  $\min_{x_1} \frac{1}{2\epsilon^2} \|y - f(x_1)\|_2^2$ . For a large class of functions  $f(\cdot)$ ,

---

**Algorithm 2** Sampling CNF with Projection-Based Guidance

---

**Require:** Trained  $u_\theta(x, t, y_1)$ , conditions  $y_1, y_2$ , projection  $P_{\Omega(y_2)}(\cdot)$ , steps  $0 = t_0 < t_1 < \dots < t_S \approx 1$  with step size  $\Delta t$

```

1: Sample  $x_0 \sim \mathcal{N}(0, 1)$ 
2: for  $i = 0, 1, \dots, S$  do
3:    $t \leftarrow t_i$ 
4:    $u_t \leftarrow u_\theta(x_t, t, y_1)$ 
5:    $\hat{x}_1 \leftarrow x_t + (1 - t)u_t$            (estimate destination)
6:    $g_t \leftarrow w_t[P_{\Omega(y_2)}(\hat{x}_1) - \hat{x}_1]$    (guidance)
7:    $x_{t+\Delta t} \leftarrow x_t + (u_t + g_t)\Delta t$ 
8: end for

```

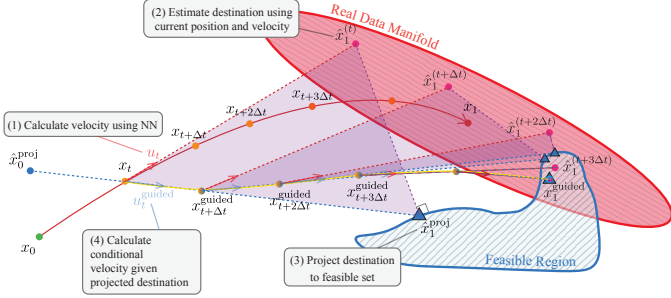


Fig. 1. Demonstration of projection-based guidance. At every step, we shift the velocity by projecting an estimation of the destination into the feasible region.

including all linear functions and some nonlinear ones (e.g., the maximum function), this problem can be solved in one step, with solution space exactly  $\Omega(y)$ . The guidance then becomes

$$g_t = b_t J_\psi^\mathcal{T}(x_t)(x_1^\star - x_1), \quad (19)$$

$$x_1^* = P_{\Omega(y)}(x_1), \quad (20)$$

where  $P_{\Omega(y)}(\cdot)$  is the projection onto  $\Omega(y)$ .

Fully evaluating  $J_\psi^T(x_t)$  in (19) requires integrating  $u_t(x_t)$  from  $t$  to 1. Following [24], we approximate with one discretization step:

$$\hat{x}_1 := x_t + (1-t)u_t(x_t), \quad (21)$$

$$J_\psi(x_t) \approx I + (1-t)J_{u_t}(x_t). \quad (22)$$

We further simplify by ignoring  $(1-t)J_{u_t}(x_t)$  in (22), as this term vanishes when  $t \rightarrow 1$  and its magnitude is typically small compared to  $I$ . The guidance reduces to

$$g_t \approx w_t[P_{\Omega(y)}(\hat{x}_1) - \hat{x}_1], \quad (23)$$

where  $w_t = \frac{1}{1-\min(t,1-\delta)}$  with  $\delta = 0.0001$  for numerical stability. The conditional velocity becomes  $u_t(x_t|y) = u_t(x_t) + \frac{P_{\Omega(y)}(\hat{x}_1) - \hat{x}_1}{1-t}$ , where the second term pulls  $\hat{x}_1$  towards the closest point in  $\Omega(y)$ .

Algorithm 2 summarizes the sampling procedure, and Fig. 1 illustrates the guidance mechanism. To combine with direct parameterization, replace  $u_\theta(x_t, t)$  with  $u_\theta(x_t, t, y_1)$  per (14). Fig. 2 shows the complete sampling process.

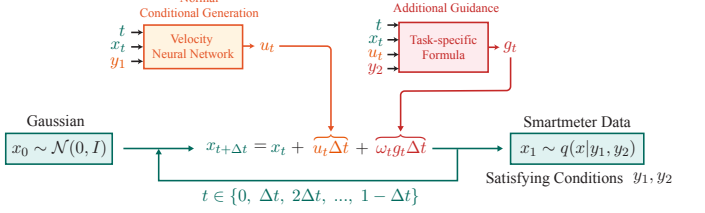


Fig. 2. Diagram of *SmartMeterFM* sampling process. The teal lines represent the data generation process, with the orange indicating the normal conditional generation part, and the red showing the additional guidance. The velocity network is a neural network.

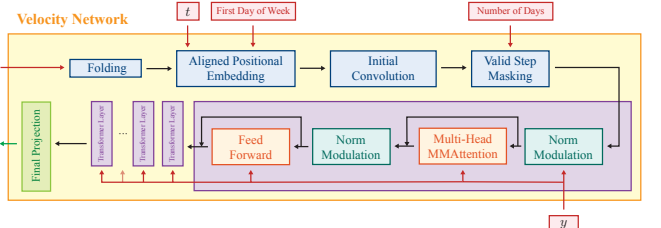


Fig. 3. Architectural design of the velocity network, as used in Fig. 2. Red arrows indicate input to the neural network, while green arrow indicates the output. The details of folding, initial convolution and final projection can be found in [9].

### III. SMARTMETERFM MODEL DESIGN

We propose *SmartMeterFM*, which builds upon the aforementioned CNF with task-specific inference time guidance. This adaptation enables the trained model to be applied to various tasks without re-training. In this section, we will first introduce the architectural design of the velocity network. Subsequently, we will demonstrate how to adapt the trained model to solve three distinct tasks: 1) generation with peak and total consumption constraints, 2) imputation, and 3) super-resolution.

## A. Architectural Design

As discussed above and as shown in Fig. 2, to sample from the CNF, we first need to parameterize  $u_\theta(x, t)$  and train the model using Algorithm 1. In this work, we parameterize it with a Transformer-based neural network. The network comprises a large-kernel convolution layer, aligned positional embedding layers, and repeated Transformer layers with valid step masking, culminating in a linear projection. The Transformer backbone is efficient in computation and has powerful temporal modeling capacity. To enable variable-length monthly profile modeling, we introduce aligned positional embedding layers and valid step masking. We also introduce a conditioning mechanism to enable effective conditioning. Fig. 3 is a diagram of the proposed velocity network. We elaborate on the specifics of these three components below. For the remaining details of the network architecture, we refer the reader to [9].

1) *Aligned Positional Embedding*: Before passing data to the Transformer blocks, we need to encode the positional information of the sequence into the sequence itself. This step is called positional embedding (encoding) [25]. Given a  $d$ -variate  $T$ -step sequence  $x \in \mathbb{R}^{d \times T}$ , for each step  $t \in$

$\{1, 2, \dots, T\}$ , we have the sinusoidal positional embedding function  $\text{PE}(t) : t \in \mathbb{N}^+ \rightarrow [-1, 1]^d$ :

$$\text{PE}_{2i}(t) = \sin\left(\frac{t}{10000^{2i/d}}\right) \quad (24)$$

$$\text{PE}_{2i+1}(t) = \cos\left(\frac{t}{10000^{2i/d}}\right), \quad (25)$$

where  $i = 1, 2, \dots, \frac{d-1}{2}$ . This function maps a time step  $t$  into a  $d$ -dimensional vector. Next, the output is passed into a multilayer perceptron (MLP) with one hidden layer:

$$\delta(t) = W_2^{\text{PE}} \text{SiLU}(W_1^{\text{PE}} \text{PE}(t) + b_1^{\text{PE}}) + b_2^{\text{PE}}, \quad (26)$$

which completes the conventional positional embedding step.

Since smart meter data exhibits strong daily and weekly periodicity, we aim to retain this information while encoding  $t$ . The above embedding is adequate when modeling daily and weekly profiles, as each  $t$  always represents the *same* intra-day or intra-week time. When modeling monthly profiles, because each month starts on a different day of the week, the  $t$  loses its synchronization with weekly periodicity. To compensate, we apply a shift to the input of positional embedding:

$$\delta'(t) = \delta(t + wT_{\text{day}}) \quad (27)$$

where  $w \in \{0, \dots, 6\}$  is the index of the first day of the week in the month,  $T_{\text{day}}$  is the number of steps per day. This simple shift ensures that the time step  $(t + wT_{\text{day}})$  is always aligned with the day of the week, facilitating the learning of the day-of-the-week pattern.

2) *Valid Step Masking*: Another major challenge of modeling a monthly profile is the varying length of each month. Fortunately, we use a Transformer that can naturally handle different sequence lengths. However, during training, it is necessary to put sequences of the same length in a batch. To circumvent this issue, we fix all profiles to have 31-day equivalent lengths. For 15 min resolution, that means each sequence has  $31 \times 96 = 2976$  steps. For months that are shorter than 31 days, we pad the end of the sequences with zeros. However, this might lead to the Attention blocks incorrectly attending to the ending zeros. Therefore, we introduce a valid step mask that blocks reading information from the invalid zeros.

For sequence  $x_{l-1} \in \mathbb{R}^{d \times T}$ , as the output of  $l-1$ -th layer and input of  $l$ -th layer, if only the first  $V \leq T$  steps are non-padded. We create a binary mask  $m \in [0, 1]^{T \times T}$

$$m_{i,j} = \begin{cases} 0 & \text{if } i \leq V \text{ and } j \leq V \\ 1 & \text{else} \end{cases}. \quad (28)$$

Next, for the Attention operation of each layer  $l \in \{1, \dots, L\}$ , and each head  $h \in \{1, \dots, H\}$ , we have

$$Q_{l,h} = W_{l,h}^q x^{(l-1)}, \quad (29)$$

$$K_{l,h} = W_{l,h}^w x^{(l-1)}, \quad (30)$$

$$V_{l,h} = W_{l,h}^v x^{(l-1)}, \quad (31)$$

We add the mask to the input of softmax function,

$$\begin{aligned} \text{Attention}_h(Q_{l,h}, K_{l,h}, V_{l,h}) \\ = V_{l,h} \text{softmax}(\text{SIM}(K_{l,h}, Q_{l,h})) \end{aligned} \quad (32)$$

$$\text{SIM}(K_{l,h}, Q_{l,h}) = \frac{K_{l,h}^T Q_{l,h}}{\sqrt{d/H}} \odot m + (-\infty) \odot (1 - m). \quad (33)$$

Here,  $\odot$  is the element-wise product. In this case, we mask the similarity function values with negative infinity wherever  $m_{i,j} = 0$ . This prevents the valid steps from attending to padded steps. Mathematically, this is equivalent to passing only the first  $V$  steps into the Transformer; however, the masking allows us to train the neural network efficiently with a batch of sequences of varying lengths.

3) *Conditioning Mechanism*: As shown in Fig. 2, to inject the information of  $y_1$  into the velocity network, we need to design a conditioning mechanism. We do this in two ways, an adaptive normalization mechanism and a multi-modal Attention (MMAttention).

In a typical Transformer layer, Layer Normalizations are used after the Attention and MLP. In our network, we add a learned modulation after the LayerNorm.

$$\text{LayerNorm}(\tilde{x}) = \frac{\tilde{x} - \mathbb{E}[\tilde{x}]}{\sqrt{\text{Var}[\tilde{x}] + \epsilon}}, \quad (34)$$

$$\lambda = W^A \text{SiLU}(W_1^A y_1 + b_1^A) + b_2^A, \quad (35)$$

$$\beta = W^B \text{SiLU}(W_1^B y_1 + b_1^B) + b_2^B, \quad (36)$$

$$\sigma = W^S \text{SiLU}(W_1^S y_1 + b_1^S) + b_2^S, \quad (37)$$

$$\tilde{x}_{\text{norm}} = \tilde{x} + \sigma \text{SubLayer}(\lambda \text{LayerNorm}(\tilde{x}) + \beta), \quad (38)$$

where  $\tilde{x}$  represents the input,  $\tilde{x}_{\text{norm}}$  the output, the  $W$  and  $b$  are learnable weights and biases, SubLayer corresponds to the feedforward layer and Attention layer, and  $\lambda, \beta, \sigma$  are modulation factors.

The MMAttention regards the condition  $y_1$  as a sequence and concatenates it with the time series sequence before performing the normal Attention operation.

$$\bar{Q}_{l,h} = W_{l,h}^q [x^{(l-1)} || y_1], \quad (39)$$

$$\bar{K}_{l,h} = W_{l,h}^w [x^{(l-1)} || y_1], \quad (40)$$

$$\bar{V}_{l,h} = W_{l,h}^v [x^{(l-1)} || y_1], \quad (41)$$

$$\text{MMAttention}_h = \text{Attention}_h(\bar{Q}_{l,h}, \bar{K}_{l,h}, \bar{V}_{l,h}). \quad (42)$$

MMAttention enables the exchange of information between the embedded time series sequence and the condition.

## B. Task Specific Guidance

In this section, we provide details on how the proposed model is adapted to solve multiple generative data tasks, namely peak-total constrained generation, imputation, and super-resolution. As described in Sec. II-D, all we need is the functional relationship between  $y$  and  $x$ ,  $y = f(x)$ . We show that this can be easily done for several tasks.

1) *Generation with peak and total consumption constraint*: Assume that we would like to generate smart meter data that satisfies some given maximum, minimum, and average value constraints. These values correspond to the monthly peak power and monthly total consumption/generation. We can write this condition as

$$y = f(x) = [\|x\|_\infty, -\| -x \|_\infty, \frac{1}{T} \mathbf{1}^T x]^T, \quad (43)$$

where  $x \in \mathbb{R}^T$  is a monthly smart meter profile,  $y$  is the stacked conditions of maximum, minimum, and average values.

2) *Imputation*: When we have partially observed smart meter data, we can use the proposed model to generate the complete smart meter data that is consistent with the observed values. Define the index set of observed values to be  $O = \{\omega_1, \dots, \omega_m\} \subset \{1, \dots, T\}$ , and the selection matrix  $S_O \in \{0, 1\}^{m \times T}$  whose  $k$ -th row is the basis vector  $e_{\omega_k}^T$ . Then

$$y = f(x) = S_O x, \quad (44)$$

which stacks all the observed values.

3) *Super-resolution*: When the measured data do not have adequate resolution, we can use the proposed model to generate higher-resolution profiles that are consistent with the measured data. Assume the measured data are the average power reading. The generated profile must have the same average when downsampled again. Assume the power readings are averaged within each  $L$ -step non-overlapping windows. Define a block-average operator  $D \in \mathbb{R}^{\frac{T}{L} \times T}$

$$D_{uv} = \begin{cases} \frac{1}{L}, & v \in \{(u-1)L+1, \dots, uL\} \\ 0, & \text{otherwise} \end{cases}. \quad (45)$$

The condition can be expressed as

$$y = f(x) = Dx. \quad (46)$$

#### IV. CASE STUDY

We evaluate the proposed method on multiple data generation tasks, detailing the dataset, tasks, and baselines below.

##### A. Dataset

We use a real dataset of approximately 350,000 monthly smart meter segments from 2022 to 2024, collected by a Dutch DSO from large customers with connections of 60 kW to 160 kW. Data are normalized to  $[-1, 1]$ , with positive values indicating consumption and negative values indicating generation. Customers are divided into 15 categories based on business type, anonymized for privacy. We focus on four categories: E3A, E3B, and E3C, which are consumption-only users, and PV, which comprises customers with large-scale solar generation.

Each monthly segment ranges from 28 days (2688 steps) to 31 days (2976 steps) at 15 min resolution, representing a challenging high-dimensional modeling task. We evaluate on January and July of each year as representative winter and summer months. The dataset is split by customer into training, validation, and test sets with a 70/15/15 ratio, ensuring no customer appears in multiple splits. The validation set is used solely for overfitting detection.

##### B. Evaluation Tasks

1) *Task 1: Generation Conditioning on Categorical Attributes*: We generate synthetic data conditioned on year, month, month length, first weekday, customer category, and generation equipment type. As these are abstract conditions,

we use only the trained conditional velocity model without inference time guidance. For evaluation, we generate 1500 samples per year, month, and customer category combination, totaling 36,000 synthetic profiles. Fidelity is assessed using the Maximum Mean Discrepancy (MMD) permutation test.

2) *Task 2: Generation Conditioning on Numerical Values*: In addition to Task 1 conditions, we specify monthly maximum, minimum, and total consumption values. We evaluate whether generated data match these numerical constraints while maintaining fidelity.

Since these detailed conditions preclude finding sufficient samples with identical conditions for MMD testing, we select 99 representative samples from the test set via k-means clustering and generate 32 samples per condition, totaling 3,168 samples. We assess performance using Continuous Ranked Probability Score (CRPS). VAE and GAN baselines are trained on these conditions, while *SmartMeterFM* uses the same model from Task 1 with guidance from (23) and (43).

3) *Task 3: Imputation*: We evaluate missing value imputation under a Missing Not at Random setting with consecutive missing blocks. Block lengths range from 5 to 595 steps, with total missing rate of 0.2.

For each of the 4 customer categories and 6 months, we select 100 representative samples via k-means clustering and generate 100 imputed candidates per sample. All baseline models are trained specifically for imputation, while *SmartMeterFM* uses the Task 1 model with guidance from (23) and (44).

4) *Task 4: Super-Resolution*: We downsample test data by averaging 16 consecutive steps, converting 15 min to 4 h resolution, then use our model to reconstruct the original 15 min profiles. Performance is evaluated using CRPS and Peak Load Error.

All baseline models are trained solely for super-resolution, while *SmartMeterFM* uses the Task 1 model with guidance from (23) and (46).

##### C. Evaluation Metrics

1) *MMD-based Permutation Testing*: Maximum Mean Discrepancy [26] measures distributional similarity in kernel space but lacks interpretable thresholds. We therefore apply a permutation test [27] following [9].

For a finite set of real data  $\mathcal{X}^{\text{real}} \sim p_1$  and synthetic data  $\mathcal{X}^{\text{synth}} \sim p_2$ , let  $z = M(\mathcal{X}^{\text{real}}, \mathcal{X}^{\text{synth}})$  denote the MMD value, where lower values indicate higher similarity. We randomly permute elements between the two sets while preserving set sizes, yielding  $\tilde{z} = M(\tilde{\mathcal{X}}^{\text{real}}, \tilde{\mathcal{X}}^{\text{synth}})$ . Under the null hypothesis  $H_0 : p_1 = p_2$ , the  $p$ -value is

$$p := \Pr[M(\tilde{\mathcal{X}}^{\text{real}}, \tilde{\mathcal{X}}^{\text{synth}}) \geq M(\mathcal{X}^{\text{real}}, \mathcal{X}^{\text{synth}}) | H_0]. \quad (47)$$

A small  $p$ -value indicates the observed MMD is unusually large, leading to rejection of  $H_0$  and suggesting distributional mismatch.

2) *Continuous Ranked Probability Score*: CRPS is a standard metric for probabilistic forecasts that generalizes Mean

Absolute Error, enabling comparison between point and probabilistic models. For a point prediction, CRPS reduces to MAE. For real data  $(x_i, y_i)$  and a probabilistic model  $\hat{p}(x|y)$ :

$$\text{CRPS}(\hat{p}(x|y_i), x_i) = \int_{\mathbb{R}} (\hat{F}_i(x) - H(x - x_i))^2 dx, \quad (48)$$

where  $\hat{F}_i$  is the CDF of  $\hat{p}(x|y_i)$  and  $H(\cdot)$  is the Heaviside step function.

3) *Peak Load Error*: Peak power information is often lost in low-resolution profiles. To evaluate peak reconstruction while mitigating outlier effects, we use the 0.9985 and 0.0015 quantiles instead of naive extrema:

$$\text{PLE}(\hat{p}(x|y_i), x_i) = \text{CRPS}(\hat{p}(Q_{0.9985}(x)|y_i), Q_{0.9985}(x_i)) + \text{CRPS}(\hat{p}(Q_{0.0015}(x)|y_i), Q_{0.0015}(x_i)), \quad (49)$$

where  $Q_\alpha(x)$  denotes the  $\alpha$ -quantile of profile  $x$ , and  $\hat{p}(Q_\alpha(x)|y_i)$  is the induced distribution obtained by sampling from  $\hat{p}(x|y_i)$ .

#### D. Baselines for Comparison

1) *Task 1*: We compare against a conditional  $\beta$ -VAE [28] with 24M parameters and a conditional WGAN [29] with 76M parameters. Both models use convolutional layers and adaptive layer normalization for condition injection, similar to our flow matching model. Both are trained until convergence.

2) *Task 2*: For deep learning baselines, we use the same  $\beta$ -VAE and WGAN models from Task 1, extended with additional conditions: monthly minimum, maximum, and average values.

For a non-deep learning baseline, we use an *algebraic scaling method*. Given a training set  $\{(x_i^{(c)}, c)\}$  where  $x_i^{(c)} \in \mathbb{R}^T$  is a profile and  $c$  is the customer category, we first compute the average profile per category:  $\bar{x}^{(c)} = \frac{1}{N_c} \sum_i x_i^{(c)}$ . To generate a profile with target maximum  $y_m$  and total consumption  $y_s$ , we normalize and scale the average profile:

$$\bar{\bar{x}}^{(c)} = \frac{\bar{x}^{(c)} - \bar{x}_{\min}^{(c)}}{\bar{x}_{\max}^{(c)} - \bar{x}_{\min}^{(c)}}, \quad (50)$$

$$\tilde{x}^{(c)}(y_s, y_m) = (\bar{\bar{x}}^{(c)})^a \cdot y_m, \quad (51)$$

where  $a$  is solved from

$$\sum_{t=1}^T (\bar{\bar{x}}_t^{(c)})^a = \frac{y_s}{y_m}. \quad (52)$$

The resulting profile  $\tilde{x}^{(c)}$  has exactly maximum value  $y_m$  and sum  $y_s$ .

3) *Task 3*: We use two baselines. First, a Masked Autoencoder [30] with a Transformer encoder-decoder architecture trained with MSE loss to predict missing values directly.

Second, we use LoadPIN [16], a GAN-based model designed for load profile inpainting. LoadPIN consists of a coarse network, a refine network, and a discriminator. We replace the original coarse network with the Masked Autoencoder Transformer described above. Following [16], we pre-train the coarse network, then freeze it and train only the refine network and discriminator adversarially. The coarse and refine networks each have approximately 2M parameters; the discriminator has 15k parameters. We use  $\lambda_1 = \lambda_2 = 0.1$  in the loss function and a learning rate of 0.001.

4) *Task 4*: We reproduce ProfileSR [19], a GAN-based super-resolution model. We use the same architecture as the original but slightly increase hidden dimensions for improved performance. The generator, discriminator, and polish networks have 507k, 23k, and 76k parameters, respectively. Training follows the two-stage procedure in [19] with a learning rate of 0.0002.

#### E. SmartMeterFM Setup

The velocity network  $u_\theta(x_t, t, y)$  has  $L = 12$  Transformer layers, model dimension  $d = 128$ , feedforward dimension  $d_{\text{ff}} = 512$ , and 7M parameters in total. We train using the Adam optimizer [31] with weight decay, a learning rate of  $10^{-4}$ , and 500k iterations, corresponding to approximately 267 epochs. Following [9], we maintain an exponential moving average (EMA) of the model weights. All baselines requiring training use the same optimizers.

For sampling, we use the EMA weights with 500 ODE discretization steps. The sampling is faster than EnergyDiff [9] due to fewer discretization steps and smaller model size.

## V. RESULTS

### A. Task 1: Generation Conditioning on Categorical Attributes

We train our proposed *SmartMeterFM* in a conditional generation setting as described in Sec. IV-B1. Table I presents the MMD permutation test results for the conditional generation task. For all categories, the average  $p$ -value across different months is above 0.05, suggesting there is no significant evidence that the approximate distribution and the real data distribution are different. Additionally, Fig. 4 shows the detailed MMD values of each category over time. The lowest (worst)  $p$ -values are 0.0570 in category E3B, July 2022 and 0.0640 in category E3C, January 2024. However, both remain above the 0.05 threshold, indicating that we accept the null hypothesis  $H_0$  in every scenario. In contrast, for VAE and GAN models, the average  $p$ -values are below 0.0001 in almost every case except for GAN in E3C. All values are below the 0.05 threshold, leading to rejection of  $H_0$ , meaning the synthetic data distributions are significantly different from the real data distribution. This gap demonstrates the superiority of flow matching models over VAEs and GANs for this task.

### B. Task 2: Generation Conditioning on Numerical Values

The *SmartMeterFM* model is trained only once for conditional generation and can be directly applied to the restricted conditional generation task. The goal is to generate smart meter data satisfying given restrictions on peak power, specifically minimum for the PV category and maximum for the other three categories, as well as monthly average values.

Table II shows the summarized CRPS for each customer category. All four evaluated methods show decent mean CRPS scores, while *SmartMeterFM* achieves the lowest. Due to the presence of a few trivial cases, such as full-zero records, the minimum CRPS of each model is nearly or exactly zero. However, for the worst-case scenarios (maximum), the CRPS varies significantly across different models and customer categories.

TABLE I

MMD PERMUTATION TEST RESULTS FOR TASK 1. THE MMD AND  $p$ -VALUES ARE CALCULATED MONTHLY AND THEN AVERAGED ACROSS MONTHS. THE  $\downarrow$  MEANS LOWER THE BETTER, AND VICE VERSA.

Model	MMD $\downarrow$	$p$ -value $\uparrow$	$p$ -value $\uparrow$ worst case
Category: E3A			
<i>SmartMeterFM</i>	0.0035	0.3925	0.2550
VAE	0.0983	< 0.0001	< 0.0001
GAN	0.0140	< 0.0001	< 0.0001
Category: E3B			
<i>SmartMeterFM</i>	0.0090	0.1612	0.0570
VAE	0.0939	< 0.0001	< 0.0001
GAN	0.0239	< 0.0001	< 0.0001
Category: E3C			
<i>SmartMeterFM</i>	0.0119	0.0945	0.0640
VAE	0.0476	< 0.0001	< 0.0001
GAN	0.0241	0.0150	< 0.0001
Category: PV			
<i>SmartMeterFM</i>	0.0042	0.5430	0.3530
VAE	0.0764	< 0.0001	< 0.0001
GAN	0.0305	< 0.0001	< 0.0001

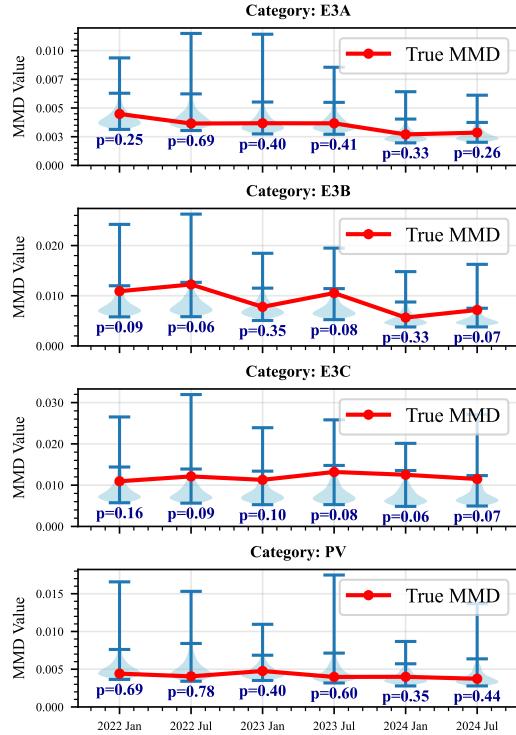


Fig. 4. MMD permutation test results of *SmartMeterFM*. Blue areas are the histograms of permuted MMD values, with the top bar indicating the maximum, the bottom bar indicating the minimum, and the middle bar indicating the 0.95 quantile. The red dots present the actual MMD value. Low MMD and high  $p$ -value suggest a small difference between the generated data and the real data.

This indicates a great diversity of the dataset. Nonetheless, *SmartMeterFM* achieves the best except in the E3B category, which is surpassed by GAN with a small margin. Overall, the scaler method has the worst CRPS. This is expected because the scaler ignores complex patterns of the data by only scaling the average profiles. Meanwhile, Table III shows the reconstruction precision on the conditioned peak and average values. The scaler method achieves 0.0000 RMSE due to its hard-coded scaling, except in the PV case, where the solution to (52) cannot be found, and only average scaling

TABLE II  
CRPS FOR GENERATION CONDITIONING ON NUMERICAL VALUES.

Method	Average $\downarrow$	Best $\downarrow$	Worst $\downarrow$
E3A			
Scaler	0.0325	0.0000	0.1492
VAE	0.0275	0.0040	0.1287
GAN	0.0241	0.0080	0.1128
<i>SmartMeterFM</i>	0.0185	0.0001	0.0988
E3B			
Scaler	0.0315	0.0000	0.1616
VAE	0.0242	0.0050	0.1172
GAN	0.0255	0.0083	0.0993
<i>SmartMeterFM</i>	0.0192	0.0002	0.1051
E3C			
Scaler	0.0545	0.0136	0.1136
VAE	0.0291	0.0085	0.0707
GAN	0.0285	0.0116	0.0582
<i>SmartMeterFM</i>	0.0190	0.0005	0.0469
PV			
Scaler	0.0460	0.0000	0.1403
VAE	0.0307	0.0048	0.0822
GAN	0.0283	0.0068	0.0881
<i>SmartMeterFM</i>	0.0213	0.0002	0.0736

TABLE III  
RMSE OF CONDITIONED MONTHLY PEAK AND AVERAGE VALUES.

Method	RMSE <sub>peak</sub> $\downarrow$	RMSE <sub>average</sub> $\downarrow$
E3A		
Scaler	0.0000	0.0000
VAE	0.1084	0.0047
GAN	0.0449	0.0175
<i>SmartMeterFM</i>	0.0177	0.0010
E3B		
Scaler	0.0000	0.0000
VAE	0.0676	0.0051
GAN	0.0433	0.0175
<i>SmartMeterFM</i>	0.0125	0.0011
E3C		
Scaler	0.0000	0.0000
VAE	0.1036	0.0056
GAN	0.0371	0.0221
<i>SmartMeterFM</i>	0.0209	0.0015
PV		
Scaler*	n.a.	0.0000
VAE	0.0548	0.0086
GAN	0.0362	0.0176
<i>SmartMeterFM</i>	0.0252	0.0014

\*: No solution was found for (52); only average scaling is used.

is employed. Among the three other models, *SmartMeterFM* always achieves the lowest RMSE, which is at least 30% lower than the second best. Meanwhile, GAN and VAE can deviate heavily from the given peak and average values.

### C. Task 3: Imputation

Table IV presents the CRPS results of the imputation task in each customer category. The ideal CRPS of 0.0000 in some cases is due to a few full-zero data points, specifically 9 out of 2,400 samples. As the impact is minor, we do not remove them from the evaluation. From Table IV, we observe that *SmartMeterFM* achieves significantly lower CRPS than the previous state-of-the-art LoadPIN, with approximately half the average CRPS in every category. Examining the maximum CRPS reveals a significant gap between the interpolation and ML-based algorithms, underscoring the need to adopt ML algorithms for the task of missing data imputation.

Fig. 5 shows one imputation example. The imputed data from Masked Autoencoder and LoadPIN are over-smoothed and heavily under-estimate the peak values (both generation and consumption). The proposed *SmartMeterFM* greatly mitigates this issue.

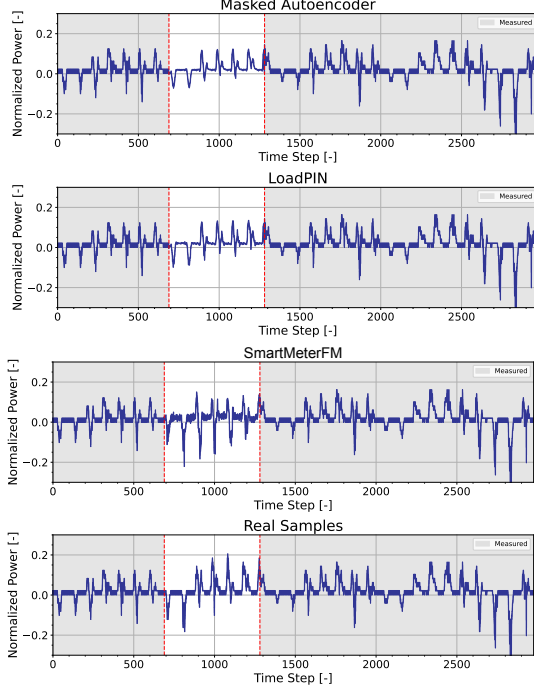


Fig. 5. Imputation results of one sample using three different approaches. The gray areas are observed while the white areas are missing, divided by the dotted red lines.

TABLE IV  
CRPS FOR IMPUTATION. LOWER IS BETTER.

Method	Average <sup>↓</sup>	Best <sup>↓</sup>	Worst <sup>↓</sup>
E3A			
Linear Interp.	0.0623	0.0000	0.2464
Nearest Neighbor Interp.	0.0694	0.0000	0.3703
Masked Autoencoder	0.0344	0.0000	0.1504
LoadPIN	0.0343	0.0010	0.2248
SmartMeterFM	0.0201	0.0015	0.1757
E3B			
Linear Interp.	0.0594	0.0000	0.3956
Nearest Neighbor Interp.	0.0618	0.0000	0.3740
Masked Autoencoder	0.0333	0.0000	0.2219
LoadPIN	0.0328	0.0010	0.1769
SmartMeterFM	0.0166	0.0015	0.1098
E3C			
Linear Interp.	0.0584	0.0000	0.2210
Nearest Neighbor Interp.	0.0624	0.0000	0.3130
Masked Autoencoder	0.0339	0.0000	0.1101
LoadPIN	0.0336	0.0002	0.1034
SmartMeterFM	0.0135	0.0018	0.0525
PV			
Linear Interp.	0.1149	0.0000	0.4023
Nearest Neighbor Interp.	0.1217	0.0000	0.4285
Masked Autoencoder	0.0507	0.0000	0.1476
LoadPIN	0.0512	0.0015	0.1587
SmartMeterFM	0.0285	0.0015	0.1171

#### D. Task 4: Super-Resolution

Table V summarizes the CRPS results of the super-resolution task. Comparing Tables IV and V, we can see that interpolation works better for the super-resolution task. This is because the large missing blocks in the imputation task are hard to recover by interpolation. Meanwhile, in super-resolution, only the high-frequency part of the data is missing. Statistically, smart meter data lie mainly on the lower-frequency components of the power spectrum. The proposed *SmartMeterFM* achieves the lowest average CRPS in each customer category, as well as the lowest worst-case CRPS. The numerical errors shown in the best-case column are also

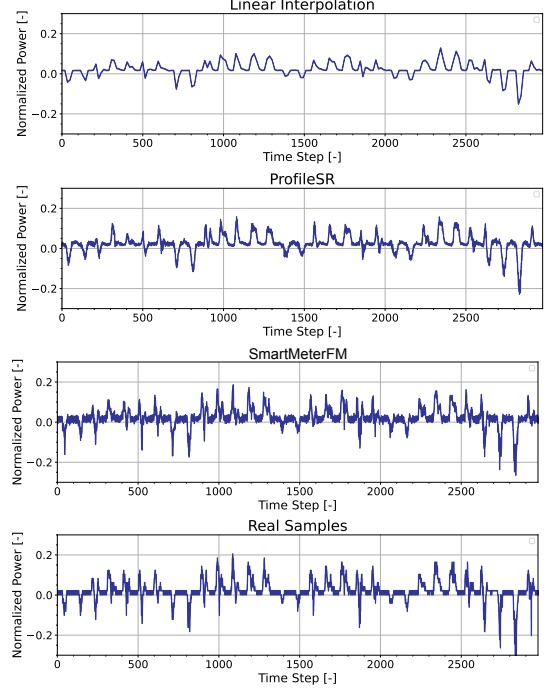


Fig. 6. 16x super-resolution results of one sample using linear interpolation, ProfileSR, and the proposed *SmartMeterFM*.

negligible.

Fig. 6 shows an example of the super-resolution data. Linear interpolation significantly underestimates the peaks and overlooks many high-frequency details. ProfileSR shows significantly better reconstruction than interpolation, but is still slightly over-smoothed. *SmartMeterFM* is qualitatively the closest to the real profile. This agrees with the quantitative results in Table V.

Additionally, because the peaks of smart meter data usually last for a short time, the information is likely to be lost in low-resolution profiles. In Table VI, we present the PLE in the reconstructed high-resolution profiles. Despite dedicated training to minimize the peak load error, ProfileSR achieved a higher PLE than our proposed *SmartMeterFM*. Moreover, our method shows substantial improvement in the most challenging PV category. Without task-specific training, our method achieves superior or comparable performance in the super-resolution task.

## VI. CONCLUSION

We propose *SmartMeterFM*, a novel Flow Matching-based model that unifies generative tasks for smart meter data. We train our model only for conditional generation and adapt it to three additional tasks without any re-training. The proposed model generates realistic data under various constraints, demonstrating superior or comparable performance in generation, peak-restricted generation, imputation, and super-resolution tasks, thereby successfully unifying these tasks with a single model.

## REFERENCES

[1] L. Cui, L. Guo, L. Gao, B. Cai, Y. Qu, Y. Zhou, and S. Yu, "A covert electricity-theft cyberattack against machine learning-based detection

TABLE V  
CRPS FOR SUPER-RESOLUTION. LOWER IS BETTER.

Method	Average $\downarrow$	Best $\downarrow$	Worst $\downarrow$
E3A			
Linear Interp.	0.0210	0.0000	0.0662
Nearest Neighbor Interp.	0.0214	0.0000	0.0652
ProfileSR	0.0187	0.0021	0.0656
SmartMeterFM	0.0124	0.0013	0.0501
E3B			
Linear Interp.	0.0193	0.0000	0.0993
Nearest Neighbor Interp.	0.0197	0.0000	0.0988
ProfileSR	0.0177	0.0015	0.0774
SmartMeterFM	0.0115	0.0013	0.0561
E3C			
Linear Interp.	0.0198	0.0000	0.0654
Nearest Neighbor Interp.	0.0200	0.0000	0.0655
ProfileSR	0.0187	0.0021	0.0657
SmartMeterFM	0.0116	0.0013	0.0549
PV			
Linear Interp.	0.0378	0.0000	0.0986
Nearest Neighbor Interp.	0.0410	0.0000	0.1110
ProfileSR	0.0334	0.0024	0.0854
SmartMeterFM	0.0201	0.0014	0.0608

TABLE VI  
PLE OF DATA AFTER SUPER-RESOLUTION. LOWER IS BETTER.

Method	Average $\downarrow$	Best $\downarrow$	Worst $\downarrow$
E3A			
Linear Interp.	0.0705	0.0000	0.4274
Nearest Neighbor Interp.	0.0604	0.0000	0.4030
ProfileSR	0.0426	0.0021	0.3635
SmartMeterFM	0.0321	0.0041	0.3873
E3B			
Linear Interp.	0.0573	0.0000	0.4078
Nearest Neighbor Interp.	0.0503	0.0000	0.3763
ProfileSR	0.0332	0.0003	0.3357
SmartMeterFM	0.0255	0.0035	0.3518
E3C			
Linear Interp.	0.0683	0.0000	0.2586
Nearest Neighbor Interp.	0.0612	0.0000	0.2470
ProfileSR	0.0382	0.0014	0.1996
SmartMeterFM	0.0248	0.0041	0.1595
PV			
Linear Interp.	0.1385	0.0000	0.5090
Nearest Neighbor Interp.	0.1198	0.0000	0.4787
ProfileSR	0.0734	0.0006	0.4154
SmartMeterFM	0.0389	0.0053	0.3962

models,” *IEEE Trans. Ind. Informat.*, vol. 18, no. 11, pp. 7824–7833, Nov. 2022.

- [2] Y. Yuan, K. Dehghanpour, F. Bu, and Z. Wang, “Outage detection in partially observable distribution systems using smart meters and generative adversarial networks,” *IEEE Trans. Smart Grid*, vol. 11, no. 6, pp. 5418–5430, Nov. 2020.
- [3] S. Maharjan, Q. Zhu, Y. Zhang, S. Gjessing, and T. Basar, “Dependable demand response management in the smart grid: A stackelberg game approach,” *IEEE Trans. Smart Grid*, vol. 4, no. 1, pp. 120–132, Mar. 2013.
- [4] M. R. Asghar, G. Dán, D. Miorandi, and I. Chlamtac, “Smart meter data privacy: A survey,” *IEEE Commun. Surveys Tuts.*, vol. 19, no. 4, pp. 2820–2835, 2017.
- [5] E. M. S. Duque, J. S. Giraldo, P. P. Vergara, P. H. Nguyen, A. van der Molen, and J. Slootweg, “Risk-Aware Operating Regions for PV-Rich Distribution Networks Considering Irradiance Variability,” *IEEE Trans. Sustainable Energy*, pp. 1–17, 2023.
- [6] E. M. S. Duque, P. P. Vergara, P. H. Nguyen, A. van der Molen, and J. G. Slootweg, “Conditional Multivariate Elliptical Copulas to Model Residential Load Profiles From Smart Meter Data,” *IEEE Trans. Smart Grid*, vol. 12, no. 5, pp. 4280–4294, Sep. 2021.
- [7] C. Wang, E. Sharifnia, Z. Gao, S. H. Tindemans, and P. Palensky, “Generating multivariate load states using a conditional variational autoencoder,” *Electr. Power Syst. Res.*, vol. 213, p. 108603, Dec. 2022.
- [8] Y. Chen, Y. Wang, D. Kirschen, and B. Zhang, “Model-free renewable scenario generation using generative adversarial networks,” *IEEE Trans. Power Syst.*, vol. 33, no. 3, pp. 3265–3275, May 2018.
- [9] N. Lin, P. Palensky, and P. P. Vergara, “EnergyDiff: Universal time-series energy data generation using diffusion models,” *IEEE Trans. Smart Grid*, vol. 16, no. 5, pp. 4252–4265, Sep. 2025.
- [10] S. Zhang, Y. Cheng, J. Qin, and N. Yu, “Generating synthetic net load data for residential customers with physics-informed diffusion models,” *IEEE Trans. Smart Grid*, pp. 1–1, 2025.
- [11] J. Lucas, G. Tucker, R. B. Grosse, and M. Norouzi, “Don’t Blame the ELBO! A Linear VAE Perspective on Posterior Collapse,” in *Advances in Neural Information Processing Systems*, vol. 32. Curran Associates, Inc., 2019.
- [12] W. Xia, H. Huang, E. M. S. Duque, S. Hou, P. Palensky, and P. P. Vergara, “Comparative assessment of generative models for transformer- and consumer-level load profiles generation,” *Sustainable Energy Grids Networks*, vol. 38, p. 101338, Jun. 2024.
- [13] S. Ben Taieb, R. Huser, R. J. Hyndman, and M. G. Genton, “Forecasting uncertainty in electricity smart meter data by boosting additive quantile regression,” *IEEE Trans. Smart Grid*, vol. 7, no. 5, pp. 2448–2455, Sep. 2016.
- [14] Y. Wang, Q. Chen, T. Hong, and C. Kang, “Review of smart meter data analytics: Applications, methodologies, and challenges,” *IEEE Trans. Smart Grid*, vol. 10, no. 3, pp. 3125–3148, May 2019.
- [15] M. Cui, J. Wang, and M. Yue, “Machine learning-based anomaly detection for load forecasting under cyberattacks,” *IEEE Trans. Smart Grid*, vol. 10, no. 5, pp. 5724–5734, Sep. 2019.
- [16] Y. Li, L. Song, Y. Hu, H. Lee, D. Wu, P. J. Rehm, and N. Lu, “Load profile inpainting for missing load data restoration and baseline estimation,” *IEEE Trans. Smart Grid*, vol. 15, no. 2, pp. 2251–2260, Mar. 2024.
- [17] L. Mai, H. Li, Y. Weng, E. Blasch, and X. Zheng, “Guaranteed conversion from static measurements into dynamic ones based on manifold feature interpolation,” *IEEE Trans. Power Syst.*, vol. 40, no. 5, pp. 3763–3777, Sep. 2025.
- [18] S. Dahale and B. Natarajan, “Recursive gaussian process over graphs for integrating multi-timescale measurements in low-observable distribution systems,” *IEEE Trans. Power Syst.*, vol. 38, no. 4, pp. 3464–3475, Jul. 2023.
- [19] L. Song, Y. Li, and N. Lu, “ProfileSR-GAN: A GAN Based Super-Resolution Method for Generating High-Resolution Load Profiles,” *IEEE Trans. Smart Grid*, vol. 13, no. 4, pp. 3278–3289, Jul. 2022.
- [20] Y. Lipman, R. T. Q. Chen, H. Ben-Hamu, M. Nickel, and M. Le, “Flow matching for generative modeling,” in *The Eleventh International Conference on Learning Representations*, Sep. 2022.
- [21] S. Chen, S. Chewi, H. Lee, Y. Li, J. Lu, and A. Salim, “The probability flow ODE is provably fast,” *Adv. Neural Inf. Process. Syst.*, vol. 36, pp. 68 552–68 575, Dec. 2023.
- [22] W. Xia, C. Wang, P. Palensky, and P. P. Vergara, “A flow-based model for conditional and probabilistic electricity consumption profile generation,” *Energy AI*, vol. 21, p. 100586, Sep. 2025.
- [23] Y. Song, J. Sohl-Dickstein, D. P. Kingma, A. Kumar, S. Ermon, and B. Poole, “Score-based generative modeling through stochastic differential equations,” in *International Conference on Learning Representations*, Oct. 2020.
- [24] H. Chung, J. Kim, M. T. Mccann, M. L. Klasky, and J. C. Ye, “Diffusion posterior sampling for general noisy inverse problems,” in *The Eleventh International Conference on Learning Representations*, Sep. 2022.
- [25] A. Vaswani, N. Shazeer, N. Parmar, J. Uszkoreit, L. Jones, A. N. Gomez, L. Kaiser, and I. Polosukhin, “Attention is All you Need,” in *Advances in Neural Information Processing Systems*, vol. 30. Curran Associates, Inc., 2017.
- [26] A. Gretton, K. M. Borgwardt, M. J. Rasch, B. Schölkopf, and A. Smola, “A kernel two-sample test,” *J. Mach. Learn. Res.*, vol. 13, no. 1, pp. 723–773, 2012.
- [27] P. Hall and N. Tajvidi, “Permutation tests for equality of distributions in high-dimensional settings,” *Biometrika*, vol. 89, no. 2, pp. 359–374, Jun. 2002.
- [28] I. Higgins, L. Matthey, A. Pal, C. Burgess, X. Glorot, M. Botvinick, S. Mohamed, and A. Lerchner, “Beta-VAE: Learning basic visual concepts with a constrained variational framework,” in *International Conference on Learning Representations*, Feb. 2017.
- [29] M. Arjovsky, S. Chintala, and L. Bottou, “Wasserstein generative adversarial networks,” in *Proceedings of the 34th International Conference on Machine Learning*. PMLR, Jul. 2017, pp. 214–223.
- [30] K. He, X. Chen, S. Xie, Y. Li, P. Dollár, and R. Girshick, “Masked autoencoders are scalable vision learners,” in *Proceedings of the IEEE/CVF Conference on Computer Vision and Pattern Recognition*, 2022, pp. 16 000–16 009.
- [31] D. P. Kingma and J. Ba, “Adam: A Method for Stochastic Optimization,” *International Conference on Learning Representations*, vol. abs/1412.6980, Dec. 2014.